Shallow subduction beneath Italy: three-dimensional images of the Adriatic-European-TyrrhenianLithosphere system based on high-quality P-wave arrival times

R. Di Stefano[1], E. Kissling[2], C. Chiarabba[1], A. Amato[1] D. Giardini[2]

R. Di Stefano, INGV, CNT, Via di Vigna Murata 605, 00143 Roma, Italy. (raffaele.distefano@ingv.it)

E. Kissling, ETH, Institute of Geophysics, Schafmattstr. 30 ETH Hoenggerberg, CH-8093 Zuerich, Switzerland. (kiss@tomo.ig.erdw.ethz.ch)

C. Chiarabba, INGV, CNT, Via di Vigna Murata 605, 00143 Roma, Italy. (claudio.chiarabba@ingv.it)

A. Amato, INGV, CNT, Via di Vigna Murata 605, 00143 Roma, Italy. (alessandro.amato@ingv.it)

D. Giardini, ETH, Institute of Geophysics, Schafmattstr. 30 ETH Hoenggerberg, CH-8093 Zuerich, Switzerland. (domenico.giardini@sed.ethz.ch)

[1]INGV, CNT, Roma, Italy

[2]ETH, Institute of Geophysics, Zuerich,

Switzerland

Abstract. This paper presents a velocity model of the Italian (central Mediterranean) lithosphere in unprecedented detail. The model is derived by inverting a set of 166,000 Pg and Pn seismic wave arrival times, restricted to the highest- quality data available. The tomographic images reveal the geometry of the subduction- collision system between the European, Adriatic, and Tyrrhenian plates, over a larger volume and with finer resolution than previous studies. We find two arcs of low-Vp anomalies running along the Alps and the Apennines, describing the collision zones of underthrusting continental lithospheres. Our results suggest that in the Apennines, a significant portion of the crust has been subducted below the mountain belt. From the velocity model we can also infer thermal softening of the crustal wedge above the subducting Adriatic plate. In the Tyrrhenian back-arc region, strong and extensive low-Vp anomalies depict upwelling asthenospheric material. The tomographic images also allow us to trace the boundary between the Adriatic and the Tyrrhenian plates at Moho depth, revealing some tears in the Adriatic-Ionian subducting lithosphere. The complex lithospheric structure described by this study is the result of a long evolution; the heterogeneities of continental margins, lithospheric underthrusting, and plate indentation have led to subduction variations, slab tears, and asthenospheric upwelling at the present day. The high-resolution model provided here greatly improves our understanding of the central Mediterranean's structural puzzle. The results of this study can also shed light on the evolution of other regions experiencing both oceanic and continental subduction.

1. Introduction

The structural setting of the central Mediterranean (Figure 1) is the result of several partly synchronous processes: oceanic subduction, continental collision, slab rollback, and back-arc basin formation [Malinverno and Ryan, 1986; Faccenna et al., 1996; Stampfli and Borel, 2002]. These processes involve the main plates of Eurasia, Adria and Africa, separated by the Mesozoic Tethys and the Permo-Triassic Neotethys oceans [Stampfli and Borel, 2002]. While there is general agreement over the opening and subduction of the Alpine Tethyan ocean, followed by a collision of plates in the Alps [e.g., Schmid et al., 2005; TRANSMED Project Working Group, 2004, and references therein], several competing models exist for the subsequent evolution of the Apennines. In particular, there is debate over whether the present setting was created by laterally continuous subduction of the Tethys and Neotethys oceanic lithospheres [Doglioni and Carminati, 2002; Faccenna et al., 2004] or by progressive detachment of the slab [Spakman andWortel, 2004]. In all models, however, the recent opening of the Tyrrhenian sea and the drift of the Calabrian arc are taken as evidence supporting the slab's broad eastward retreat.

Several questions as to the nature of this puzzling scenario remain open.

(1) What are the geometries, limits and natures of the lithospheres involved?

(2) To what extent is the asthenosphere upwelling in the eastern and southern Tyrrhenian regions?

(3) Is the entire Adriatic lithosphere currently subducting, and is this process laterally continuous?

(4) Is there thermal softening of the Apennines wedge?

(5) What can we learn about the strength of the continental lithosphere? The answers to

these questions will also be relevant to our general understanding of continental subduction and collision processes. The availability of a large, high-quality data set of P wave arrival times makes this tectonicallycomplex Mediterranean region one of the best choices for achieving general insights into the subduction/collision process. This paper presents high-quality images of the lithosphere- asthenosphere system in the central Mediterranean. We compute a three-dimensional velocity model using the highest-quality P wave arrival times from local and regional earthquakes. The new data set is created by the automated repicking [Di Stefano et al., 2006] of the Istituto Nazionale di Geofisica e Vulcanologia (INGV) seismic catalogue [Chiarabba et al., 2005]. The consistently weighted and selected Pg and Pn wave arrivals enable us to resolve lithospheric structures as small as 15-30 km in the crust, or 30-60 km in the uppermost mantle (up to 80 km in depth). We invert our data set using a modified version of the code originally developed by Zhao et al. [1992, 1994], which models sharp velocity discontinuities such as the crust-mantle boundary within a 3-D grid of nodes. The lithosphere velocity structure is thus revealed with fine definition, as is the plate boundary at Moho depths. Our results provide new insights into the tectonics and geodynamic evolution of the region, as well as general information relevant to similar subduction/collision orogeny.

2. Tectonic setting

The evolution of the Alps and the Apennines has been described by Dewey et al. [1989], Doglioni and Carminati [2002], Speranza and Chiappini [2002], Faccenna et al. [2004], Schmid et al. [2005], Ganne et al. [2006], and Lucente et al. [2006], among many others. From here on out, the nomenclature "Adriatic plate" comprises bothAdria (in its sensu strictu) in the north and Apulia in the south. We use "Alpine Tethys" and

"Neotethys" to refer to the Ligure-Provenzale and Ionian oceans, respectively [Stampfli and Borel, 2002]. [7] Around 80 Ma ago, the Mesozoic Alpine Tethys began to close owing to convergence of the African and European plates [Capitanio and Goes, 2006, and references therein]. South vergent subduction of the Alpine Tethys ocean began at 85 Ma [Babist et al., 2006], followed by continental collision of Adria and Europe around 40 Ma. The postcollisional shortening has continued until today, leading to the formation of the Alpine chain. The Apennines formed more recently (starting about 35 Ma ago) as a consequence of two processes: subduction of the southwesternmost part of the Neotethys ocean, and slab retreat leading to asymmetric opening of the Tyrrhenian sea (12-10 Ma to present) [Faccenna et al., 2004; Chiarabba et al., 2008]. Presently enclosed in the central Mediterranean, this region has evolved into a jigsaw puzzle of irregular plates and fragmented slabs. [8] Seismic tomography provides key information on the upper mantle structure. Remnant lithosphere slabs (with high Vp) and traces of former subduction have been found by inverting regional and teleseismic data beneath the Alps [Lucente et al., 1999; Lippitsch et al., 2003; Piromallo and Morelli, 2003], the northern Apennines, and the southern Tyrrhenian sea [Amato et al., 1993; Spakman et al., 1993; Ciaccio et al., 1998; Lucente et al., 1999; Cimini and De Gori, 2001; Piromallo and Morelli, 2003; Montuori et al., 2007]. [9] Although the lateral and vertical continuity of the subducting slabs is reasonably well defined below 100 km, the shallow geometry of the colliding plates is still unresolved. [10] Regional seismological studies [Mele et al., 1998; Di Stefano et al., 1999; Piromallo and Morelli, 2003] have yielded first-order information on the lithosphereasthenosphere system and blurred images of an anomalous low-Vp belt beneath the Italian peninsula. These studies were hampered by the limited

amount and poor consistency of available seismic bulletin data. [11] Further constraints on crustal thickness, Moho geometry, and mean crustal P wave velocities were obtained using controlled source seismology (CSS) [Ye et al., 1995; Pialli et al., 1998; Finetti et al., 2001; TRANSALP Working Group, 2002; Scrocca et al., 2003], which is capable of resolving significant local details even lacking information on the lateral continuity of modeled features. More recently, studies using the receiver functions (RF) method [Piana Agostinetti et al., 2002; Mele and Sandvol, 2003] have further constrained the geometry of the subduction system by measuring the crustal thickness along some transects of the Apennines. The extensive use of SKS splitting analysis at broadband seismic stations has permitted researchers to define the mantle's deformation and kinematics [Margheriti et al., 2003; Lucente et al., 2006]. In the Apennines, several such works have revealed the existence of three distinct domains (European, Tyrrhenian, and Adriatic) characterized by distinct yet internally consistent fast SKS directions. Lucente et al. [2006] propose that the fast directions are a direct signature of the Ionian slab retreat. Baccheschi et al. [2007], on the other hand, think they are a marker of toroidal flow around the retreating Ionian slab. [12] Tomographic and SKS splitting studies provide significant constraints on the structure and kinematics of the upper mantle, mainly furnishing results at depths of 100-150 km and below. Our investigation focuses on theshallow part of the lithosphere, whose structure is still poorly known.

3. Tomographic Inversion

3.1. Data

To obtain high-resolution velocity images, we use a large data set of high-quality P wave arrival times. This is the first time such a sample has been constructed for Italy. Drawing

on the entire catalogue of local and regional earthquakes recorded by the INGV since 1988 [Di Stefano et al., 2006], the data are selected by an advanced, automated system with error estimation capabilities [Aldersons, 2004]. A certain number of high-quality, hand-picked arrival times from other permanent seismic networks operating in the region are also added. [14] We first locate the seismic events using HYPOELLIPSE [Lahr, 1999] and a minimum 1-D velocity model [Chiarabba et al., 2005]. From the initial set of 39,616 INGV events, we selected the 8206 earthquakes (Figure 2a) with location errors 5 km in x, y, and z; azimuthal gap 180 ; 1-D location RMS 0.6 s; a minimum of 15 P wave arrivals; and focal depths ranging from near the surface to 100 km. The data set includes 166,000 Pg and long-distance Pn observations, recorded at about 600 stations (Figure 2b). The coverage provided by these data is sufficient to ensure excellent and fairly homogeneous sampling of the study volume down to 80 km in depth. The estimated average observation error is 0.2s. Data are weighted according to the uncertainty in the readings, following a scheme laid out by Di Stefano et al. [2006].

3.2. Method

We use the inversion code originally developed by Zhao et al. [1992], as modified by Di Stefano and Chiarabba [2002]. This technique has been successfully applied in regional [Zhao et al., 1992, 1994; Di Stefano et al., 1999] and very local seismic tomography studies [Zhao and Kanamori, 1993; Di Stefano and Chiarabba, 2002]. This iterative procedure uses the LSQR algorithm by Paige and Saunders [1992] to solve for hypocentral and velocity parameters, and continues as long as the misfit between model and data is significant. The LSQR algorithm allows us to use a very large arrival time data set and constrain thousands of model parameters, at the cost of not computing the inverse

matrix. Consequently, model resolution needs to be verified with synthetic tests. An amplitude damping parameter is used to balance model complexity (number of parameters) against data misfit (RMS error). At each iteration the damping parameter is recalculated and updated to optimize this trade-off (Figure 3a).Seismic raypaths are traced using a combination of two approaches: a pseudobending method in continuous regions of the velocity model, and Snell's law at discontinuities such as the Moho [Zhao et al., 1992; Zhao and Kanamori, 1993]. Velocity values are assigned and modified on a 3-D grid, but the geometry of the discontinuity is fixed. P wave velocities along the raypaths are calculated by linear interpolation between nearest nodes. The wavelength corresponding to the dominant frequency of first arrivals (Figure 3b) is approximately 6 km, suggesting that the minimum distance between adjacent nodes should be 8- 10 km. To find the best parameterization consistent with our data, we progressively decreased the horizontal grid spacing from 30 km to 10 km, with a layer every 15 km, and performed sensitivity tests on checkerboard-like velocity models. The 15 km grid provides good image fidelity and resolution while adequately sampling the entire region. The entire grid consists of two layers in the crust, a flat Moho at 34 km, and four layers in the upper mantle down to 80 km. The Moho depth is an average of several published values. The effect of this choice on the results has been investigated and discussed in a previous work [Di Stefano et al., 1999]. [17] The chosen grid size is about twice the dominant wavelength, so is small enough to gain a reasonably detailed 3-D image of the lower crust and upper mantle. The distribution of raypaths is fairly even over most of the region, and the ratio between the number of observations and the number of unknown model parameters is very high. Thus, even this relatively dense grid is well sampled. [18] For the first iteration, P wave

velocities are taken from Chiarabba and Frepoli [1997] and the JB model [Jeffreys and Bullen, 1940] for the crust and uppermost mantle, respectively (see reference velocities in Figure 5). In subsequent iterations, seismic rays are traced through the 3-D velocity model. Most of the Moho undulations strike across the Apennines belt, so the constant Moho has little effect on long-distance Pn waves, which travel mostly along the range's axis. [19] Figure 3b shows an example of rays traced for a single event, specifically the first and last iterations. To get more stable results, we inverted only those nodes hit by more than 50 rays. This resulted in 11,200 model parameters to be estimated. Stations are modeled at their true elevations. After only four iterations, with a damping parameter of 45, we achieve a variance reduction of 74[20] F test would allow one more iteration but from the fifth iteration on additional variance reduction is 3the previous one. We thus prefer to be conservative and we stop the iterative procedure at the fourth iteration. [21] The weighted residuals RMS decreases from its starting value of 0.98 s to 0.50 s at the fourth iteration. Weighted RMS is obtained by taking into account the quality of P phase readings, according to

RMS where rn and wn are the residual and normalized weight of the nth P phase, respectively. To further reduce the RMS, we would have to reduce the grid spacing. This would increase the number of model parameters at the cost of locally degraded model resolution. As uniform model resolution is of pivotal importance to reducing geometrical distortions and other artifacts in the tomographic images [Kissling et al., 2001], we prefer not to sacrifice uniformity for the sake of enhancing local details. Rather, we maintain a good formal resolution of velocity parameters throughout the model, with a grid suitable for lithosphere imaging and avoiding higher model complexity. [22] The mean horizontal

and vertical hypocenters' shifts are '2 km and '4 km, respectively, after the earthquakes are relocated. We do not observe a significant correlation between earthquake depth and the origin time adjustment. The stability of the 3-D hypocenters can be attributed to the high quality of the arrival times in our data set, and the robustness of our solution to the coupled hypocentervelocity problem.

3.3. Model resolution

In order to estimate model reliability, we performed several synthetic tests computing travel times in structures known a priori. Gaussian distributed noise with a standard deviation of 0.3 s, 1.5 times larger than the estimated uncertainty of our data set [Di Stefano et al., 2006], is added to the data and then synthetic travel times are reweighted accordingly. In addition to the classic checkerboard structure, we use a structure of large tiles to obtain more complete information on the confidence level of our tomographic images. In both tests, the synthetic anomalies are 10Figure 4 shows the results of synthetic tests performed with damping according to the preferred model. In areas where the geometry of the synthetic anomalies is well reproduced, 80[24] In the 8 km layer, the resolution is good. Both geometry and amplitude are recovered for structures 30 km wide (Figures 4a and 4b). Large, irregular structures are well reproduced, but amplitude recovery is incomplete in some locations. High resolution is achieved along thepeninsula and in the Alps but not in the Po plain. This result is expected given the seismic network coverage. [25] In the 22 km layer, resolution is very good for structures 30 km wide, with characteristics similar to those described for the previous layer (Figures 4c and 4d). [26] In the 38 km layer, resolution is excellent for structures 30 km wide. The amplitudes and geometries of all synthetic anomalies are recovered over a large area, larger than that

seen in any other layer (Figures 4e and 4f). At this depth the geometry of the Adriatic, Tyrrhenian, and European plates is best defined. [27] In the 52 km layer, despite some evidence of NW-SE smearing effects, we resolve large structures (60 km to 100 km wide) over almost the entire layer (Figures 4g and 4h). At such resolutions, plate geometry and boundaries can still be reliably defined. [28] In the 66 km layer, the resolution is fair only for structures as wide as 200 km (Figure 4j). Because of the predominantly horizontal sampling by Pn raypaths, the velocity model suffers from leakage of the anomalies trending NW-SE. However, we nicely resolve across-strike (NE-SW) discontinuities such as the boundary between the Adriatic and the Tyrrhenian plates. [29] In the 80 km layer, the resolution is poor over most of this layer, except for a small volume located in the Calabrian arc where even sampling is guaranteed by both Pn rays and intersecting steep rays from intermediate-depth events (z 100 km) of the southern Tyrrhenian subduction zone (Figures 4k and 4l).In Figure 4m we present four vertical sections, cuts through the large-scale (60 km) checkerboard test corresponding to sections B, E, G, and H of Figure 6. Even though there is little vertical leakage between the layers, the synthetic anomalies are well reproduced within the most heavily sampled regions of the inverted volume. [31] A comparison with our earlier results in the work by Di Stefano et al. [1999] demonstrates strong improvement in the resolution of the crust, mainly owing to the higher quality of the data. By using consistently weighted longdistance Pn arrivals, we were also able to extend the resolved volume down to 80 km depth. [32] To further verify the model's potential resolution, we have computed a restore test. In this test the synthetic model is the 3-D model of the preferred inversion. The result of this test shows very good recovery of both low- and highfrequency anomalies. (Restore test results are available

online as auxiliary material.)1 The synthetic tests just described support the reliability of the real velocity anomalies discussed in the section 4. [33] Analysis of the inversion process (Figure 3) indicates that a damping parameter of 45 is appropriate for our data and model parameterization. Nevertheless, our model (hereafter called the preferred model) still exhibits some highfrequency perturbations and a pronounced roughness. Roughness may be suspicious in certain locations, however, and high-frequency perturbations have no straightforward interpretation in the mantle. Thus, we ran a second inversion of the data using the much higher and very conservative damping parameter of 100 (see Figure 3). This model is very smooth, showing only the most robust velocity anomalies. The obvious cost is that it deamplifies the absolute variations. After 4 iterations, this overdamped model achieves a final weighted RMS of 0.54 s and a variance improvement of 70are somewhat less than those seen in the preferred model. We note that the two models correspond very well, again testifying to the high quality of the data set. We base our interpretation and discussion mainly on the most robust features, those also revealed in the overdamped solution. Local and small-scale anomalies of the preferred inversion are considered important only in the most well-resolved regions of the model.

4. Three-Dimensional P Wave Velocity Model

Inversion results for the overdamped and preferred solutions are shown in Figure 5. In the upper and lower crust, the tomographic model shows very strong, localized, lateral heterogeneities (DVp = 15mantle structure is dominated by continuous anomalies, with large Vp perturbations on the order of 4-10Overall, we observe much complexity in the velocity images reflecting small-scale variations in the tectonics of the Alps and Apennines. [35] We shall focus our discussion on those first-order features which are resolved

in both inversions, and their relation to the main elements of Alpine and Apennine tectonics. In this section, we describe and interpret the anomalies observed in each layer and vertical section individually, postponing their geodynamic implications until section 5. Our structural interpretation is based on the current literature for P wave velocities in the crust and uppermost mantle [Mavko, 1980; Christensen and Mooney, 1995] and is constrained by independent geological and geophysical information.In the upper crust (8 km depth), the recovered P wave velocity pattern accurately reflects large-scale local geology. The highs correspond to known limestone or crystalline basement units, and the lows to recent sedimentary basins. The velocity anomalies recovered by the preferred inversion are consistent with previous tomographic models obtained from dense local networks [e.g., Chiarabba et al., 1995; Chiarabba and Amato, 1997]. In particular, low-Vp anomalies due to thick sedimentary deposits are found along the Apennine foredeeps and intramountain extensional basins (Figure 5). The largest sedimentary basin in the region, the Po Plain, is not detected as a low-Vp anomaly due to the sparse network geometry. An extensive low-Vp anomaly is observed beneath the Neapolitan area (see Figure 1), however, possibly related to thick layers of sedimentary rock from the Mount Vesuvius and Campi Flegrei Quaternary volcanoes. Along the south Alpine and Apennine belts, high-Vp anomalies are found in coincidence with the internal and foreland limestone platform units of the Adria-Africa continental margin.In the 22 km layer, we find two strong high-Vp anomalies in the western Alps. These features are related to the Ivrea-Verbano body and the shallow Ligurian upper mantle. The rest of the Alpine belt is characterized by broad, low-Vp anomalies, which we interpret as material of the upper crust underthrusting the belt. These anomalies correspond to previously identified structures [Waldhauser

et al.,2002]. Along the Apennines, we find a continuous low-Vp zone following the mountain belt axis. [38] In the 38 km layer beneath the Alps and the Apennines, we find a broad, continuous, low-velocity anomaly that mirrors the arcuate shape of the belt (see Figure 1). These perturbations have an amplitude of about 10implying P wave velocities that are inconsistent with those of mantle rocks [Christensen and Mooney, 1995]. We interpret these low-Vp belts as subducting crustal material. [39] On the Tyrrhenian side of the Apennines we observe isolated low-Vp regions (anomalies on the order of 4-6most of which coincide with Quaternary volcanoes or geothermal regions. We interpret these features as thermal anomalies in the Tyrrhenian mantle, in agreement with the existence of volcanism and the observed high heat flow [Barberi et al., 1973; Mongelli et al., 1989; Ventura et al., 1999; Marani and Trua, 2002; Zito et al., 2003]. Our findings in this layer also confirm the existence of substantial crustal thickening beneath the Alps, as observed in previous studies [see, e.g., Menard and Thouvenot, 1984; Geiss, 1987; Kissling, 1993; Ye et al., 1995; TRANSALP Working Group, 2002]. [40] At greater depths (52 to 66 km), low-Vp anomalies are found in the western and eastern Alps, indicating an underthrust of lower crust material. In the Apennines, the two negative velocity features found at 38 km (i.e., the Adriatic crustal material and the hot Tyrrhenian mantle) join to generate a broad, low-Vp anomaly. To the east, this anomaly faces an elongated region of positive P wave velocities related to the cold, down bending Adriatic lithospheric mantle. Along the Apennines we find some disruptions of this high-Vp belt, which could represent local tears in the subducting lithosphere (referred to as slab windows in the following discussion). [41] At depths of 80 km, a 70 km wide arc of high velocities (from +2Arc to the northern Apennines. This feature represents the subducting Adriatic mantle lithosphere. Although

the resolution of the model is low at depths greater than 52 km, the presence of this feature in both inversions suggests vertical continuity of the subducting lithosphere, at least in the Calabrian Arc. [42] All of the velocity anomalies described above are present in both inversions, so they may be considered robust, first-order heterogeneities. [43] To clarify the geometry of the lithosphereasthenosphere system beyond that visible in the maps of Figure 5, we now discuss vertical sections through the velocity model (Figure 6). These velocity images are compared with independent results on crustal structure obtained from CSS experiments [see Maistrello and Musacchio, 2003, and references therein; Scrocca et al., 2003]. In general, we find striking similarities between the two. The horizontally layered initial velocity model is shown in the inset of Figure 6. Its velocities range from 5.0 km/s inthe upper crust to about 8.0 km/s at 80 km depth. The Moho is marked by the transition between yellow and red, the former depicting the lower crust.

4.1. Deep structure of the Alps

The most prominent feature beneath the Alpine belt is a lateral, continuous, low-Vp anomaly at 38 km showing the European and Adriatic continental, crustal material forming the belt roots (Figure 5). In the crust of western Alps, there is a NNE oriented finger of exceptionally high Vp (7.0-7.2 km/s, see Figure 5 and section A of Figure 6), consistent with a strong positive Bouguer anomaly [Coron, 1963; Menard and Thouvenot, 1984]. This local maximum is generated by high-grade, metamorphic, basic and ultrabasic rocks forming the so-called Ivrea-Verbano structure, which is the exhumed mantle of the Adriatic microplate [Schmid and Kissling, 2000; Schmid et al., 2005]. Its role in the geodynamic evolution of the region will be described in section 5.4. [45] In vertical section B (Figure 6), along the European Geotraverse (EGT) profile [Valasek et al., 1991; Ye et

al., 1995], we identify three high-Vp anomalies corresponding to the European, Adriatic and Tyrrhenian mantle lithospheres. In this section we can clearly observe the relationship between the Alps and the Apennines. The European lithosphere is underthrusting the Adriatic plate (X = 150-250 km, section B), in agreement with the interpretations of Ye et al. [1995] and Schmid et al. [2005]. From 300 to 400 km along section B and from 0 to 60 km along section C, we observe low-velocity anomalies at depths of 38 and 52 km (see also Figure 5). These data suggest that the Adriatic crust is underthrusting the Tyrrhenian mantle to the south.The high-Vp anomaly of the Adriatic mantle is interrupted by a prominent negative velocity anomaly (X = 220-250 km, section B), which does not appear to be an artifact. The negative anomaly is also visible in the overdamped solution, and our resolution tests indicate that a feature of this size should be reliable. The low-Vp anomaly could originate from a torsion of the plate induced by its subduction beneath the Apennines. [47] In the eastern Alps, the relationship between the European and Adriatic plates is controversial [TRANSALP Working Group, 2002; Kummerow et al., 2004; Lippitsch et al., 2003; Schmid et al., 2005]. Results from CSS [TRANSALP Working Group, 2002] and migrated receiver functions [Kummerow et al., 2004] suggest that the European Moho underthrusts the Adriatic lithosphere to the south. On the other hand, high-resolution teleseismic tomography [Lippitsch et al., 2003] reveals that a high-velocity body connected to the Adriatic lithosphere is subducting northeast beneath the European plate [see also Schmid et al., 2005]. Our model shows that the Adriatic lithosphere deepens from 30 to 50 km toward the axis of the Alpine belt (X = 350-250 km in section D), while the European mantle lithosphere dips southward in a similar way

(X = 80-200 kmin section C). Unfortunately, our model cannot determine which of these is the overriding plate.

4.1.1. Northern Apennines. The main feature in the northern Apennines is a broad, continuous belt of low Vp values (at 38 km depth) along the length of the range (Figure 5), indicating that material of the Adriatic crust is being subducted. In the central Apennines this anomaly widens and extends to the east, suggesting crustal thickening and possibly a high mantle temperature. Sections E and F in Figure 6 show that the high-Vp Adriatic lithosphere is subducting beneath the warmer, low-Vp Tyrrhenian lithosphere over the entire Italian peninsula. Portions of the continental crust remain attached to the mantle lid, leading to the belt-shaped, low-Vp anomaly. [49] Section E runs along the Crosta Profonda (CROP03) near-vertical reflection profile [Pialli et al., 1998] and describes a region where much CSS data are available [Maistrello and Musacchio, 2003]. The Adriatic mantle lithosphere is characterized by high velocities (Vp 8.0 km/s) and shows a gentle southwestward dip. The Adriatic Moho, identified by a sudden transition from 7.5 km/s to 8.0 km/s, lies at depths corresponding to those revealed by past CSS data. The base of the lower crust is deflected from about 35 to 60 km depth (X = 120-225 km in section E, X 100 to 180 in section F). This result confirms previously published structural models derived from active [Pialli et al., 1998] and passive seismological records [Piana Agostinetti et al., 2002; Mele and Sandvol, 2003] and extends their results to greater depths. In the westernmost margin (X = 0-35 km) of section E, the high- Vp anomaly between 38 km and 52 km corresponds to strong and deep reflections of the CROP03 profile. Our findings may support the hypothesis that this anomaly traces a relic of the European lithosphere [Pauselli et al., 2006]. [50] A vast, low-Vp zone pervades the

volume between the Tyrrhenian and Adriatic lithospheres. Beneath the Tyrrhenian side of the Apennines, the mantle velocities in our model are significantly lower than the normal range of 7.9- 8.0 km/s [Mavko, 1980; Christensen and Mooney, 1995; Mooney et al., 1998]. When such low-Vp values are considered along with the shallow Moho depth determined from receiver function studies [Piana Agostinetti et al., 2002; Mele and Sandvol, 2003], the anomalous heat flow of the region [Mongelli and Zito, 2000], and S wave attenuation [Mele et al., 1997; Marone et al., 2004], evidence points to a significant crustal extension and asthenosphere upwelling [Mongelli et al., 1989; Carmignani and Kligfield, 1990; Jolivet et al., 1990]. This extension thins the crust that was previously thickened by formation of the Alpine belt (whose relic could be the high-Vp anomaly in section E) and Plio-Quaternary volcanism.

4.1.2. Southern Apennines. In the southern Apennines, a small segment (about 160 km) of the subducting Adriatic mantle is clearly visible in between two slab windows of the central and southern Apennines (labeled CAWand SAWin Figure 5). The lateral extent of this segment is consistent with the positive mantle anomaly described by Chiarabba et al. [2008], which was interpreted as the oceanic portion of the slab. The southernmost section (G) shows that the Adriatic high-Vp mantlelithosphere is almost flat beneath the Apulian region, but dips steeply to the southwest in correspondence with the mountain range. The southernmost slab window (SAW) is located near a tear between the Ionian and Adriatic slabs, which was recently proposed using slab velocity and attenuation models [Chiarabba et al., 2008]. The tear is located at the boundary between the oceanic Ionian lithosphere and the Adriatic continental lithosphere.

4.1.3. Calabrian Arc. Velocity anomalies in this region are reliably resolved down to 80 km (section H, Figure 6) thanks to an abundance of intermediate-depth seismic events. Our results reveal the top of the subducted Ionian lithosphere as a high- Vp anomaly located about 40 km beneath Calabria, gently (about 30) dipping to the NW from the Tyrrhenian coast to the Eolian Islands. At greater depths, this anomaly joins with a steep high-Vp slab imaged by global and teleseismic tomography [Amato et al., 1993; Spakman et al., 1993; Lucente et al., 1999; Piromallo and Morelli, 2003; Spakman and Wortel, 2004; Montuori et al., 2007; Chiarabba et al., 2008]. Positive Vp anomalies in the mantle and intermediate to deep earthquakes define the NW subducting slab down to a depth of 500 km [Anderson, 1987; Giardini and Velona, 1991; Selvaggi and Chiarabba, 1995; Frepoli et al., 1996; Montuori et al., 2007; Finetti, 2005; Chiarabba et al., 2008]. On top of the high-Vp slab, a narrow, low-Vp belt reveals the presence of subducting crustal material.

4.1.4. Tyrrhenian domain. The main feature in this region is the presence of low-Vp anomalies at depths of 22, 38, and 52 km (see Figure 5). The deepest anomaly is also the most pronounced. These results reflect strong thermal anomalies in the lower crust and indicate that the lithosphere and asthenosphere upwellings are destabilizing. The phenomenon is more pronounced beneath the southern Tyrrhenian back-arc region, where we observe a diffuse low-velocity anomaly consistent with the upwelling of asthenospheric material. Melted mantle rises in the lower crust, feeding the magmatism of the volcanic arc of the Eolian Islands and the Marsili Seamount spreading center [Marani and Trua, 2002] (see Figure 5). The flowing asthenosphere extends to the peri- Tyrrhenian margin of the Apennines. At depths of 38 and 22 km, the anomalies are narrow and closely associated

382 with the roots of the Quaternary volcanoes, the magmatic provinces of Tuscany, Latium
383 and Campania, and the Aeolian Islands (Figure 1).

5. Geodynamic implications

384 The present structure of the Alps and Apennines derives from the closure of the Tethys
385 and Neotethys oceans, two events that occurred at different times, followed by a collision
386 between the continental margins of Europe, Adria, and Africa. Our results help identify
387 the geometry and boundaries of the plates, and also provide some constraints on the nature
388 of the lithosphere. These interpretations will be described in the following sections. [55]
389 Our first remarkable result is the definition of the limit of the Adriatic slab, which runs
390 from the northern Apennines to Sicily (see Figure 7). On the basis of velocityanomalies in
391 the upper mantle, we can infer that subduction of the Neotethys ocean has not taken place
392 along the entire belt. In particular, we find two slab windows in the central and southern
393 Apennines (labeled CAW and SAW, respectively, in Figure 5). A third may be present
394 in the northern Apennines, although this feature is less robust. We support the idea that
395 these windows were generated by tears in the Adriatic/Ionian slab during its progressive
396 rollback, promoted by complexity in the subducting continental lithosphere and/or trench
397 elongation [Govers and Wortel, 2005; Chiarabba et al., 2008]. These regions lack positive
398 velocity anomalies in the mantle [Lucente et al., 1999; Chiarabba et al., 2008; Rosenbaum
399 et al., 2008] and intermediate depth seismicity [Chiarabba et al., 2005; Cadoux et al.,
400 2007],and their magma geochemistry deviates from that typical of subduction zones. The
401 progressive development of slab tears has recently been proposed to explain the complex
402 evolution of several subduction zones, including the central Mediterranean [Lallemand
403 et al., 2001; Levin et al., 2002; Govers and Wortel, 2005; Miller et al., 2006; Chiarabba

et al., 2008]. Once a slab tear is generated, the decreased slab width may favor sudden acceleration of the retreat and an ultrafast opening of the back-arc region, as has been observed for the Ionian slab [Faccenna et al., 2004; Nicolosi et al., 2006; Chiarabba et al., 2008]. Our findings thus complement the model of slab evolution proposed by Schellart et al. [2007], specifically by adding data on mixed oceanic-continental subduction zones.

5.1. Upraising of the Tyrrhenian asthenosphere

The broad, low-Vp volume located from 38 km downward in the Tyrrhenian sea and along the western margin of the Apennines is a very robust feature appearing in both the preferred and the overdamped inversions. This structure clearly delineates the extent of the upraised asthenosphere (Figures 5 and 6). In the northern Apennines, the same upwelling is confined inland and represents a reasonable source for the diffuse high heat flow [Mongelli and Zito, 2000] and CO2 degassing observed by Chiodini et al. [2004]. Consistent with this interpretation, the pervasive Quaternary magmatism and intrusions found beneath geothermal sites in this region [Barberi et al., 1973; Serri et al., 1993; Chiarabba et al., 1995] all developed above the asthenospheric upwelling. The low-Vp anomaly observed at 22 km beneath the mountain region (see Figure 5 and section F, at X = 60-90) suggests that the asthenospheric wedge is associated with strong thermal effects, in agreement with a negative Bouguer anomaly of deep crustal origin [Tiberti et al., 2005]. In the central Apennines the asthenosphere widens and extends eastward, flowing inside the CAW slab window. In the southern Apennines, the asthenosphere extends as far east as the mountain belt. These data agree with the shallow Tyrrhenian Moho (24-26 km) revealed by CSS [Scrocca et al., 2003; Finetti, 2005] and receiver function analysis [Steckler et al., 2008]. The bulk of the asthenospheric upwelling is located underneath

426 the Tyrrhenian sea, and the negative anomalies are consistent with the geometry of the
427 oceanic Marsilii basin inferred from geomagnetic data [Nicolosi et al., 2006]. [57] Magma
428 upwelling fed volcanism in the back-arc region, and fragmented the Tyrrhenian plate (see
429 section H in Figure 6). Isolated volumes of very low Vp are present at the crust-mantle
430 interface underneath most of the Quaternary volcanoes, alternating with high-Vp spots
431 which are relics of the collisional belt. Relative to the northern Apennines, the Tyrrhenian
432 plate in this region has been more extensively substituted by oceanic material. This can
433 be attributed to a more vigorous and prolonged rollback of the Neotethys slab during the
434 Plio-Pleistocene [Faccenna et al., 2002; Cifelli et al., 2007; Chiarabba et al., 2008].

5.2. What is subducting beneath the Apennines?

435 The low-Vp belt imaged at 38 km along the northern Apennines reveals that a significant
436 portion of the crust (at least the whole lower crust) is subducting beneath the Apennines,
437 along with the Adriatic mantle lid definedby the high-Vp anomaly. The high-Vp mantle
438 (Figure 6) has the same westward dip of the regional monocline as defined by Mariotti and
439 Doglioni [2000]. The lateral extent of the low-Vp anomaly at 38 km and the curvature of
440 the plate observed in vertical sections (Figure 6, sections E, F, and G) both indicate that
441 the dip of the Adriatic plate changes as one moves along the peninsula. From the central
442 Apennines southward, the low-Vp anomaly related to the subducted crust vanishes, and
443 the continuity of the high-Vp Adriatic mantle is broken (at 38 and 52 km, respectively,
444 see Figure 5). The change in dip and loss of continuity in the subducted lithosphere
445 may be explained by a lateral variation of the Adriatic crust thickness, derived from
446 early Mesozoic dismemberment of the passive margin and the early Triassic rift episodes
447 documented by Grandic and Samarzija [2002]. We suppose that the subduction of this

laterally heterogeneous lithosphere, along with the irregular and still unknown extent of the Neotethys ocean [Stampfli and Borel, 2002], may have produced significant variations in the flexure and subduction of the crust thereby leading to the development of slab tears.

5.3. Thermal softening of the Apennine wedge

Consistent with our previous work [Di Stefano et al., 1999], we find elongated low-Vp bands in the lower crust of the Apennine wedge (22 km layer in Figure 5). These perturbations can be as strong as 8-10absolute P wave velocities less than 5.5 km/s. Note that such velocities are inconsistent with all rock types that can be reasonably expected in the lower crust. We therefore interpret this feature as a thermal softening of the crust originated by the underlying asthenosphere. It is also possible that the low velocities derive from deep fluids released by the downgoing slab [Kirby et al., 1996; Kawakatsu and Watada, 2007]. It is interesting to note, however, that the affected volume closely coincides with the normal faulting belt in the upper crust [Chiarabba et al., 2005], indicating that the two processes are related. The presence of heated and/or fluid-filled volumes beneath the Apennines may play a significant role in localizing the active extension and developing the normal fault belt.

5.4. What have we learned about the strength of the continental lithosphere?

Several features of the model suggest that the Adriatic lithosphere is quite strong. The first observation is that a portion of the Adriatic crust is subducting along with the mantle lid in the northern Apennines. The decollement layer between subducted and accreted material is therefore located within the crust. This process places significant stress on the

descending plate and leads to flexure of the Adriatic upper crust, giving rise to locally thick fore-deep successions [Royden et al., 1987]. Further evidence for the strength of the Adriatic lithosphere may be found in its fragmented regions and slab windows, both of which indicate a rigid response to the subduction process. Finally, the rigid frontal part of the continental Adriatic lithosphere (i.e., the high-Vp Ivrea-Verbano exhumed mantle) is strongly indented into the western Alps. As a result, both the crust and the upper mantle are severely deformed (see section A, Figure 6). The indentation of the Ivrea-Verbano Body is a key element in the evolution of the Alps and Apennines. It seems to havehampered the underthrusting of continental material and the development of the south verging south Alpine belt in the western and central Alps. Conversely, the south Alpine belt is well developed in the eastern central Alps. Thus, the indentation created flexure in the Adriatic plate beneath the Apennines and possibly led to its torsion and breakup as well. Evidence for this is visible as a well-resolved, robust low-Vp anomaly at 52 km (see Figure 5 and section A of Figure 6). All of these features emphasize the strength of the Adriatic lithosphere, and show that the complexities observed at the surface and in the uppermost crust also extend to the upper mantle.

5.5. The Tyrrhenian-Adriatic plate boundary

Velocity images and other geophysical data [Pialli et al., 1998; Piana Agostinetti et al., 2002; Mele and Sandvol, 2003] indicate that the Tyrrhenian crust is thin (18-26 km), dips slightly to the east, and overlies a low-Vp asthenospheric body. The Tyrrhenian crust is reasonably constituted by crustal material scraped off the subducting Adriatic plate, and to the west by the former European lithosphere. The high-Vp anomaly observed 38 km under the western side of Tuscany (section E, Figure 6) is consistent with the

deep seismic reflectors revealed by the CROP03 program. These were attributed to the European crust [see also Pauselli et al., 2006]. During the late Tertiary, the Tyrrhenian plate experienced stretching and diffuse extension following the rollback of the Adriatic lithosphere [Faccenna et al., 2004] and asthenosphere upwelling. [62] We can identify the boundary between the Adriatic- Ionian and Tyrrhenian plates at Moho depth by tracing the western limit of the low-Vp anomalies related to underthrusting continental material at a depth of 38 km (Figure 7) and by considering the Moho geometry determined in previous studies [Barchi et al., 1998; De Franco et al., 2000; Piana Agostinetti et al., 2002; Mele and Sandvol, 2003; Piana Agostinetti and Amato, 2009]. The plate boundary approximately follows the regional divide (Figure 7b) rather than the culmination of the surface topography. A possible explanation is that the drainage pattern is controlled by the dynamic support to the topography, as proposed by D'Agostino and McKenzie [1999] on the basis of gravimetric data. [63] The active normal faulting belt (see Figure 2a and Chiarabba et al. [2005]) is consistently located along the plate boundary. In the northern Apennines and Calabrian Arc, our plate boundary is consistent with the division defined by Margheriti et al. [2003] between the Adriatic and Tyrrhenian domains in the mantle based on SKS splitting. However, we find some discrepancies in the central Apennines. It is possible that the presence of the CAW prevents us from defining a clear plate boundary in this part of the Adriatic slab.

6. Conclusions

This paper has presented a new, high-resolution Vp model revealing the geometry of the central Mediterranean region's European, Adriatic, and Tyrrhenian plates. As a considerable amount of high-quality, passive seismic data is available for this region, this

analysis will help us understand how the competition between oceanic and continental subduction plays out in detail. We propose that heteroge-

514 **Acknowledgments.** We are grateful to C. Doglioni and D. Scrocca for stimu-
515 lating discussions about the geodynamicsof the central Mediterranean region. W.
516 Spakman, S. Goes, and an anonymous Associate editor providedvery useful com-
517 ments for strengthening the paper. We used Vincenzo Liberatore's "Gauss random
518 generator"(http://vorlon.cwru.edu/∼vxl11/) to produce random Gaussian noise, GMT
519 [*Wessel and Smith*, 1995]to generate all the figures and perform some computing tasks,
520 and many other tools created by theOpen Source worldwide community. This work was
521 partly supported by the GNDT project *Terremoti Probabili in Italia 2000-2030*, coord. A.
522 Amato and G. Selvaggi,funded by the *Dipartimento Protezione Civile* (DPC) of Italy.

References

Alder sons, F. (2004), Toward three-dimensional crustal structure of the Dead Sea region from local earthquake tomography, Ph.D. thesis, Tel Aviv University, Israel, http://faldersons.net.

Amato, A., B. Alessandrini, G. Cimini, A. Frepoli, and G. Selvaggi (1993), Active and remnant subducted slabs beneath Italy: evidence from seismic tomography and seismicity, *Ann. Geofis.*, *36*, 201– 214.

Anderson, H. (1987), The deep seismicity of the Tyrrhenian Sea, *Geophys. J. Int.*, *91*, 613–637.

Babist, J., M. R. Handy, M. Konrad-Schmolke, and K. Hammerschmidt (2006), Precollisional, multistage exhumation of subducted continental crust: The sesia zone, western alps, *Tectonics*, *25*(6), doi:10.1029/2005TC001,927.

Baccheschi, P., L. Margheriti, and M. Steckler (2007), Seismic anisotropy reveals focused mantle flow around the Calabrian slab (southern Italy), *Geophys. Res. Lett.*, *34*(5), L05,302.

Barberi, F., P. Gasparini, F. Innocenti, and L. Villari (1973), Volcanism of the southern Tyrrhenian Sea and its geodynamic implications, *J. Geophys. Res.*, *78*(23), 5221–5232.

Barchi, M., G. Minelli, and G. Pialli (1998), The CROP 03 profile: a synthesis of results on deep structures of the northern Apennines, *Mem. Soc. Geol. It.*, *52*, 383–400.

Cadoux, A., J. Blichert-Toft, D. Pinti, and F. Albaréde (2007), A unique lower mantle source for southern italy volcanics, *Earth Planet. Sci. Lett.*, *259*(3-4), 227– 238.

Capitanio, F., and S. Goes (2006), Mesozoic spreading kinematics: consequences for Cenozoic central and western Mediterranean subduction, *Geophys. J. Int.*, *165*(3), 804–816.

Carmignani, L., and R. Kligfield (1990), Crustal extension in the northern Apennines - the transition from compression to extension in the Alpi Apuane core complex, *Tectonics*, *9*(6), 1275–1303.

Chiarabba, C., and A. Amato (1997), Upper crustal structure of the benevento area (southern Italy): fault heterogeneities and potential for large earthquakes, *Geophys. J. Int.*, *130*, 229- -239.

Chiarabba, C., and A. Frepoli (1997), Minimum 1D velocity models in central and southern Italy: a contribution to better constrain hypocentral determinations, *Ann. Geofis.*, *40*(4), 937–954.

Chiarabba, C., A. Amato, and A. Fiordelisi (1995), Upper crustal tomographic images of the Amiata-Vulsini geothermal region, central Italy, *J. Geophys. Res.*, *100*(B3), 4053–4066.

Chiarabba, C., L. Jovane, and R. Di Stefano (2005), A new global view of Italian seismicity using 20 years of instrumental recordings, *Tectonophysics*, *395*, 251– 268.

Chiarabba, C., P. De Gori, and F. Speranza (2008), The Southern Tyrrhenian subduction zone: Deep geometry, magmatism and Plio-Pleistocene evolution, *Earth Planet. Sci. Lett.*, *268*(3-4), 408–423.

Chiodini, G., C. Cardelli, A. Amato, E. Boschi, S. Caliro, and F. Frondini (2004), Carbon dioxide earth degassing and seismogenesis in central and southern Italy, *Geophys. Res. Lett.*, *31*, doi:10.1029/2004GL019,480.

Christensen, N., and W. Mooney (1995), Seismic velocity structure and composition of the continental crust; a global view, *J. Geophys. Res.*, *100*(B6), 9761– 9788.

567 Ciaccio, M., G. Cimini, and A. Amato (1998), Tomographic images of the upper mantle
568 high-velocity anomaly beneath the northern Apennines, *Mem. Soc. Geol. It.*, *52*, 353–
569 364.

570 Cifelli, F., F. Rossetti, and M. Mattei (2007), The architecture of brittle postorogenic
571 extension: Results from an integrated structural and paleomagnetic study in north
572 Calabria (southern Italy), *Bull. Geol. Soc. Am.*, *119*(1/2), 221– 239.

573 Cimini, G., and P. De Gori (2001), Nonlinear P-wave tomography of subducted lithosphere
574 beneath central-southern Apennines (Italy), *Geophys. Res. Lett.*, *22*(23), 4387– 4390.

575 Coron, S. (1963), *Apercu Gravimetrique sur les Alpes Occidentales: Année geophysique*
576 *internationale*, vol. 12, CNRS, Paris.

577 D'Agostino, N., and D. McKenzie (1999), Convective support of long-wavelength topog-
578 raphy in the Apennines (Italy), *Terranova*, *11*, 234–238.

579 De Franco, R., G. Biella, G. Caielli, A. Corsi, A. Mauffret, I. Contrucci, and A. Nercessian
580 (2000), Interpretation of wide angle reflection refraction data in the Tuscan-Latium peri-
581 Tyrrhenian area, *Boll. Soc. Geol. It.*, *119*, 171– 188.

582 Dewey, J., H. Helman, E. Turco, D. Hutton, and S. Knott (1989), *Kinematics of the*
583 *western Mediterranean*, pp. 265– 283, in Alpine Tectonics, M.P. Coward and D. Dietrich
584 and R.G. Park.

585 Di Stefano, R., and C. Chiarabba (2002), Active source tomography at mt.
586 vesuvius: Constraints for the magmatic system, *J. Geophys. Res.*, *107*(B11),
587 doi:10.1029/2001JB000,792.

588 Di Stefano, R., C. Chiarabba, F. Lucente, and A. Amato (1999), Crustal and upper-
589 mostmantle structure in Italy from the inversion of P-wave arrival times: geodynamic

implications, *Geophys. J. Int.*, *139*, 483–498.

Di Stefano, R., F. Aldersons, E. Kissling, C. Chiarabba, and D. Giardini (2006), Automatic seismic phase picking and consistent observation error assessment: application to Italian seismicity, *Geophys. J. Int.*, *165*(1), 121– 134.

Doglioni, C., and E. Carminati (2002), The effects of four subductions in the NE- Italy, *Mem. Soc. Geol. It.*, *54*, 1– 4.

Faccenna, C., P. Davy, J. Brun, R. Funiciello, D. Giardini, M. Mattei, and T. Nalpas (1996), The dynamics of back-arc extension: an experimental approach to the opening of the Tyrrhenian Sea, *Geophys. J. Int.*, *126*, 781– 795.

Faccenna, C., F. Speranza, F. D. Caracciolo, M. Mattei, and G. Oggiano (2002), Extensional tectonics on Sardinia (Italy): insights into the arc-back-arc transitional regime, *Tectonophysics*, *356*, 213–232.

Faccenna, C., C. Piromallo, A. Crespo-Blanc, L. Jolivet, and F. Rossetti (2004), Lateral slab deformation and the origin of the western Mediterranean arcs, *Tectonics*, *23*, TC1012, doi:10.1029/2002TC001,488.

Fine tti, I. (Ed.) (2005), *Crustal section based on CROP seismic data across the North Tyrrhenian-Northern Apennines-Adriatic Sea*, 794 pp., Elsevier.

Finetti, I., M. Boccaletti, M. Bonini, A. D. Ben, R. Geletti, M. Pipan, and F. Sani (2001), Crustal section based on CROP seismic data across the north Tyrrhenian- northern Apennines-Adriatic Sea, *Tectonophysics*, *343*, 135–163.

Frepoli, A., G. Selvaggi, C. Chiarabba, and A. Amato (1996), State of stress in the southern Tyrrhenian subduction zone from fault-plane solutions, *Geophys. J. Int.*, *125*(3), 879–891.

Ganne, J., D. Marquer, G. Rosenbaum, J. Bertrand, and S. Fudral (2006), Partitioning of deformation within a subduction channel during exhumation of high-pressure rocks : a case study from western Alps, *J. Struct. Geol.*, *28*(7), 1193– 1207.

Geiss, E. (1987), A new compilation of crustal thickness data for the Mediterranean area, *Ann. Geophys.*, *5B*(6), 623–630.

Giardini, D., and M. Veloná (1991), The deep seismicity of the Tyrrhenian Sea, *Terranova*, *3*, 57–64.

Govers, R., and M. Wortel (2005), Lithosphere tearing at STEP faults; response to edges of subduction zones, *Earth Planet. Sci. Lett.*, *236*(1-2), 505–523.

Grandic, S., and M. B. J. Samarzija (2002), Geophysical and stratigraphic evidence of the Adriatic Triassic rift structures, *Mem. Soc. Geol. It.*, *57*(1), 315– 325.

Jeffreys, H., and K. Bullen (1940), *Seismological tables*, British Association for the Advancement of Science.

Jolivet, L., R. Dubois, M. Fournier, B. Goffe, A. Michard, and C. Jourdan (1990), Ductile extension in Alpine Corsica, *Geology*, *18*(10), 1007–1010.

Kawakatsu, H., and S. Watada (2007), Seismic evidence for deep-water transportation in the mantle, *Science*, *316*(1468), doi: 10.1126/science.1140,855.

Kirby, S., S. Stein, E. Okal, and D. Rubie (1996), Metastable mantle phase transformations and deep earthquakes in subducting oceanic lithosphere, *34*(2), 261– 306.

Kissling, E. (1993), Deep structure of the Alps: what do we really know?, *Phys. Earth planet. Int.*, *79*, 87–112.

Kissling, E., S. Husen, and F. Haslinger (2001), Model parametrization in seismic tomography: a choice of consequence for the solution quality, *Phys. Earth planet. Int.*, *123*,

89–101.

Kummerow, J., R. Kind, O. Oncken, P. Giese, T. Ryberg, K. W. amd F. Scherbaum, and TRANSALP Working Group (2004), A natural and controlled source seismic profile through the eastern Alps: TRANSALP, *Earth Planet. Sci. Lett.*, *225*(1-2), 115- -129.

Lahr, J. (1999), Hypoellipse: A computer program for determining local earthquake hypocentral parameters, magnitude, and first-motion pattern (y2k compliant version), *U.S.G.S. Open File Report*, *99-23*.

Lallemand, S., Y. Font, H. Bijwaard, and H. Kao (2001), New insights on 3-d plates interaction near taiwan from tomography and tectonics implications, *Tectonophysics*, *335*, 229– 253.

Levin, V., N. Shapiro, J. Park, and M. Ritzwoller (2002), Seismic evidence for catastrophic slab loss beneath kamchatka, *Nature*, *418*(6899), 763–767.

Lippitsch, R., E. Kissling, and J. Ansorge (2003), Upper mantle structure beneath the Alpine orogen from high-resolution teleseismic tomography, *J. Geophys. Res.*, *108*(B8), 2376. doi:10.1029/2002JB002,016.

Lucente, F., C. Chiarabba, G. Cimini, and D. Giardini (1999), Tomographic constraints on the geodynamic evolution of the Italian region, *Geophys. Res. Lett.*, *104*, 20,307–20,327.

Lucente, F., L. Margheriti, C. Piromallo, and G. Barruol (2006), Seismic anisotropy reveals the long route of the slab through the western-central Mediterranean mantle, *Earth Planet. Sci. Lett.*, *241*(3-4), 517– 529.

Maistrello, M., and G. Musacchio (2003), Archiving seismic r/war data from Italy and surrounding seas, *Geophys. Res. Abs.*, *5*, 1235.

Malinverno, A., and W. Ryan (1986), Extension in the Tyrrhenian Sea and shortening in the Apennines as result of arc migration driven by sinking of the lithosphere, *Tectonics*, *5*, 227–245.

Marani, P., and T. Trua (2002), Thermal constriction and slab tearing at the origin of a superinflated spreading ridge: Marsilii volcano (Tyrrhenian Sea), *J. Geophys. Res.*, *107*(B9), 2188, doi:10.1029/2001JB000,285.

Margheriti, L., F. Lucente, and S. Pondrelli (2003), Sks splitting measurements in the Apenninic-Tyrrhenian domain (Italy) and their relation with lithospheric subduction and mantle convection, *J. Geophys. Res.*, *108*(B4), 2218, doi:10.1029/2002jb001,793.

Mariotti, G., and C. Doglioni (2000), The dip of the foreland monocline in the Alps and Apennines, *Earth Planet. Sci. Lett.*, *191*, 191–202.

Marone, F., S. van der Lee, and D. Giardini (2004), Three-dimensional upper-mantle s-velocity model for the Eurasia-Africa plate boundary region, *Geophys. J. Int.*, *158*(1), 109– 130.

Mavko, M. (1980), Velocity and attenuation in partially molten rocks, *J. Geophys. Res.*, *85*(B10), 5173–5189.

Mele, G., and E. Sandvol (2003), Deep crustal roots beneath the northern Apennines inferred from teleseismic receiver functions, *Earth Planet. Sci. Lett.*, *211*, 69– 78.

Mele, G., A. Rovelli, D. Seber, and M. Barazangi (1997), Shear wave attenuation in the lithosphere beneath Italy and surrounding regions: Tectonics implications, *J. Geophys. Res.*, *102*(B6), 11,863–11,875.

Mele, G., A. Rovelli, and D. Seber (1998), Compressional velocity structure and anisotropy in the uppermost mantle beneath Italy and surrounding regions, *J. Geophys. Res.*,

682 *103*(B6), 12,529– 12,543.

683 Ménard, G., and F. Thouvenot (1984), Ecaillage de la lithosphère Européenne sous les
684 Alpes occidentales: arguments gravimétriques et sismiques liés á l'anomalie d'Ivrea,
685 *Bull. Soc. Gèol. Fr.*, *26*, 875– 884.

686 Miller, M., A. Gorbatov, and B. L. N. Kennett (2006), Three-dimensional visualization of
687 a nearvertical slab tear beneath the southern mariana arc, *Geochem. Geophys. Geosyst.*,
688 *7*, doi:10.1029/2005GC001,110.

689 Mongelli, F., and G. Zito (2000), The thermal field in a basin after a sudden passive
690 pure shear lithospheric extension and sublithospheric mechanical erosion: the case of
691 the Tuscan Basin (Italy), *Geophys. J. Int.*, *142*(1), 142– 150.

692 Mongelli, F., G. Zito, N. Ciaranfi, and P. Pieri (1989), Interpretation of heat flow density
693 of the apennine chain, Italy, *Tectonophysics*, *164*, 267–280.

694 Montuori, C., G. Cimini, and P. Favali (2007), Teleseismic tomography of the southern
695 Tyrrhenian subduction zone: New results from sea-floor and land recordings, *J. Geo-*
696 *phys. Res.*, *112*(B03311, doi:10.1029/2005JB004114).

697 Mooney, W., G. Laske, and T. Masters (1998), Crust 5.1: a global crustal model at 5 5,
698 *J. Geophys. Res.*, *103*, 727,747.

699 Nicolosi, I., F. Speranza, and M. Chiappini (2006), Ultrafast oceanic spreading of the
700 marsili basin, southern Tyrrhenian Sea: Evidence from magnetic anomaly analysis,
701 *Geology*, *34*(9), 717–720; doi: 10.1130/G22,555.1.

702 Paige, C. C., and M. A. Saunders (1992), Lsqr: An algorithm for sparse linear equations
703 and sparse least squares, *ACMTMS*, *8*, 43–71.

Pauselli, C., M. Barchi, C. Federico, B. Magnani, and G. Minelli (2006), The crustal structure of the northern Apennines (central Italy); an insight by the CROP03 seismic line, *Am. J. Sci.*, *306*(6), 428–450.

Pialli, G., M. Barchi, and G. Minelli (1998), Results of the CROP03 deep seismic reflection profile, *Mem. Soc. Geol. It.*, *52*, 654.

Piana Agostinetti, N., F. Lucente, G. Selvaggi, and M. Di Bona (2002), Crustal structure and moho geometry beneath the northern Apennines (Italy), *Geophys. Res. Lett.*, *29*(20), doi:10.1029/2002gl015,109.

Piromallo, C., and A. Morelli (2003), P-wave tomography of the mantle under the Alpine-Mediterranean area, *J. Geophys. Res.*, *108*(B2), doi:10.1029/2002JB001,757.

Rosenbaum, G., M. Gasparon, F. Lucente, A. Peccerillo, and M. Miller (2008), Kinematics of slab tear faults during subduction segmentation and implications for italian magmatis, *Tectonics*, *27*(2), doi:10.1029/2007TC002,143.

Royden, L., E. Patacca, and P. Scandone (1987), Segmentation and configuration of subducted lithosphere in Italy: an important control on thrust-belt and foredeep-basin evolution, *Geology*, *15*(8), 714– 717.

Schellart, W., J. Freeman, D. Stegman, L. Moresi, and D. May (2007), Evolution and diversity of subduction zones controlled by slab width, *Nature*, *446*, 308- -311.

Schmid, S., and E. Kissling (2000), The arc of the western Alps in the light of geophysical data on deep crustal structure, *Tectonics*, *19*(1), 62–85.

Schmid, S., B. Fügenschuh, E. Kissling, and R. Schuster (2005), Tectonic map and overall architecture of the Alpine orogen, *Eclogae geol. Helv.*, *97*, 93–117.

726 Scrocca, D., C. Doglioni, F. Innocenti, P. Manetti, A. Mazzotti, L. Bertelli, L. Burbi,
727 and S. D'Offizi (Eds.) (2003), *CROP ATLAS - Seismic Reflection Profiles of the Italian*
728 *Crust*, *Mem. Descr. Carta. Geol. It.*, vol. 62.

729 Selvaggi, G., and C. Chiarabba (1995), Seismicity and P-wave velocity image of the south-
730 ern Tyrrhenian subduction zone, *Geophys. J. Int.*, *121*, 818– 826.

731 Serri, G., F. Innocenti, and P. Manetti (), Geochemical and petrological evidence of
732 the subduction of delaminated Adriatic continental lithosphere in the genesis of the
733 Neogene-Quaternary magmatism of central Italy, *Tectonophysics*, *223*, 117– 147.

734 Spakman, W., and R. Wortel (2004), *A tomographic view on the Western Mediterranean*
735 *geodynamics*, pp. 31–52, in The TRANSMED Atlas. The Mediterranean Region from
736 Crust to Mantle, Springer- Verlag.

737 Spakman, W., S. van der Lee, and R. van der Hilst (1993), Travel-time tomography of
738 the European- Mediterranean mantle down to 1400 km, *Phys. Earth planet. Int.*, *79*,
739 3–74, doi:10.1016/0031-9201(93)90142- V.

740 Speranza, F., and M. Chiappini (2002), Thick-skinned tectonics in the external Apennines,
741 Italy; new evidence from magnetic anomaly analysis, *J. Geophys. Res.*, *107*(B11), 19,
742 doi:10.1029/2000JB000027.

743 Stampfli, G., and G. Borel (2002), A plate tectonic model for the paleozoic and meso-
744 zoic constrained by dynamic plate boundaries and restored synthetic oceanic isochrons,
745 *Earth Planet. Sci. Lett.*, *196*, 17–33.

746 Steckler, M., N. Piana Agostinetti, C. Wilson, P. Roselli, L. Seeber, A. Amato, and
747 A. Lerner-Lam (2008), Crustal structure in the southern Apennines from teleseismic
748 receiver functions, *Geology*, *36*, 155–158.

Tiberti, M., L. Orlando, D. Di Bucci, M. Bernabini, and M. Parotto (2005), Regional gravity anomaly map and crustal model of the central southern Apennines (Italy), *J. Geodyn.*, *40*, 73– 91.

TRANSALP Working Group (2002), First deep seismic reflection images of the eastern Alps reveal giant crustal wedges and transcrustal ramps, *Geophys. Res. Lett.*, *29*(10), 1452, 10.1029/2002GL014,911.

TRANSMED Project Working Group (2004), *The TRANSMED Atlas: geological-geophysical fabric of the Mediterranean region - Final report of the project*, vol. 27, 244-254 pp.

Valasek, P., F. Mueller, and K. Holliger (1991), Results of nfp 20 seismic reflection profiling along the Alpine section of the European geotraverse (egt), *Geophys. J. Int.*, *105*, 85--102.

Ventura, G., G. Vilardo, G. Milano, and N. Pino (1999), Relationships among crustal structure, volcanism and strike-slip tectonics in the Lipari-Vulcano volcanic complex (Aeolian Islands, southern Tyrrhenian sea, Italy), *Phys. Earth planet. Int.*, *116*, 31–52.

Waldhauser, F., R. Lippitsch, E. Kissling, and J. Ansorge (2002), High-resolution teleseismic tomography of upper-mantle structure using an a priori three-dimensional crustal model, *Geophys. J. Int.*, *150*, 403–414.

Wessel, P., and W. H. F. Smith (1995), New version of the Generic Mapping Tools released, *EOS Trans. Am.*, *76*, 329.

Ye, S., J. Ansorge, E. Kissling, and S. Mueller (1995), Crustal structure beneath the eastern Swiss Alps derived from seismic refraction data, *Tectonophysics*, *242*, 199–221.

771 Zhao, D., and H. Kanamori (1993), The 1992 Landers earthquake sequence; earthquake
772 occurrence and structural heterogeneities, *Geophys. Res. Lett.*, *20*(11), 1083–1086.
773 Zhao, D., A. Hasegawa, and S. Horiuchi (1992), Tomographic imaging of P- and S-wave
774 velocity structure beneath northeastern Japan, *J. Geophys. Res.*, *97*(B13), 19,909–
775 19,928.
776 Zhao, D., A. Hasegawa, and H. Kanamori (1994), Deep structure of Japan subduction
777 zone as derived from local, regional and teleseismic events, *J. Geophys. Res.*, *99*(B11),
778 22,313– 22,329.
779 Zito, G., F. Mongelli, S. de Lorenzo, and C. Doglioni (2003), Heat flow and geodynamics in
780 the Tyrrhenian Sea, *Terranova*, *15*(doi: 10.1046/j.1365-3121.2003.00507.x), 425– 432.

781

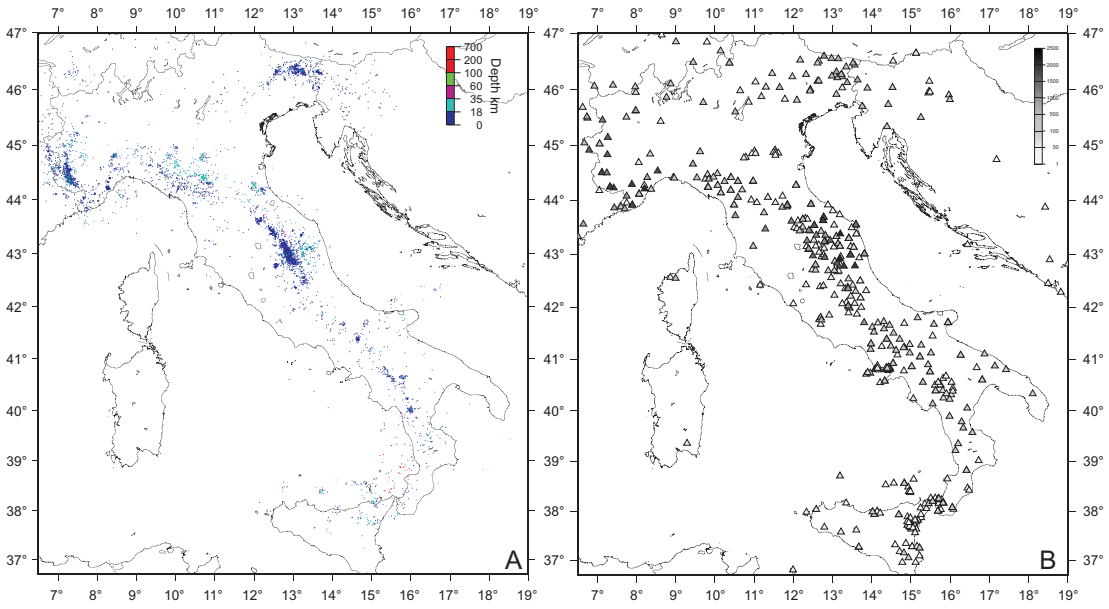

782

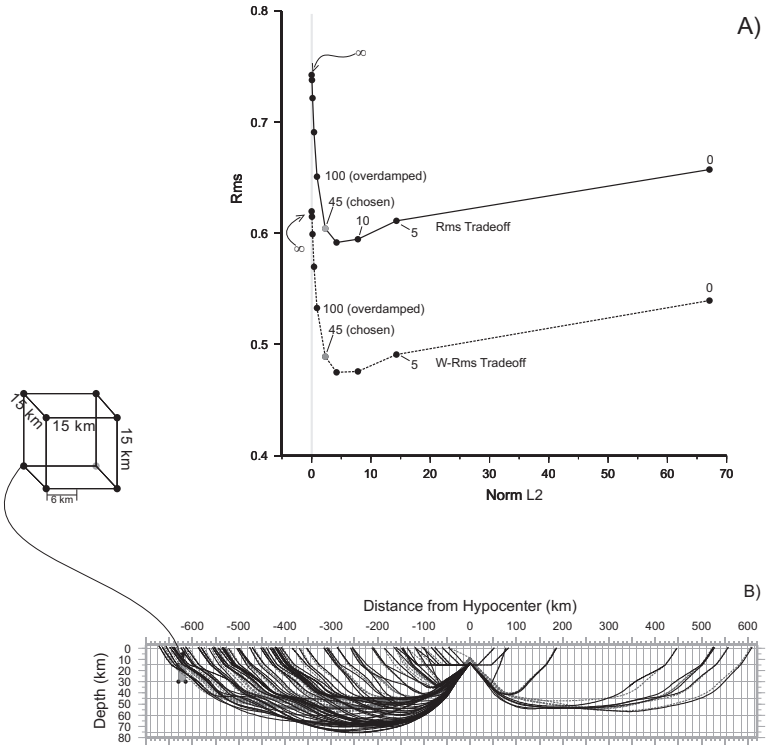
A)
Rms
Norm L2
100 (overdamped)
45 (chosen)
10
5
0
Rms Tradeoff
W-Rms Tradeoff
15 km
15 km
15 km
6 km
B)
Distance from Hypocenter (km)
Depth (km)

Figure 3

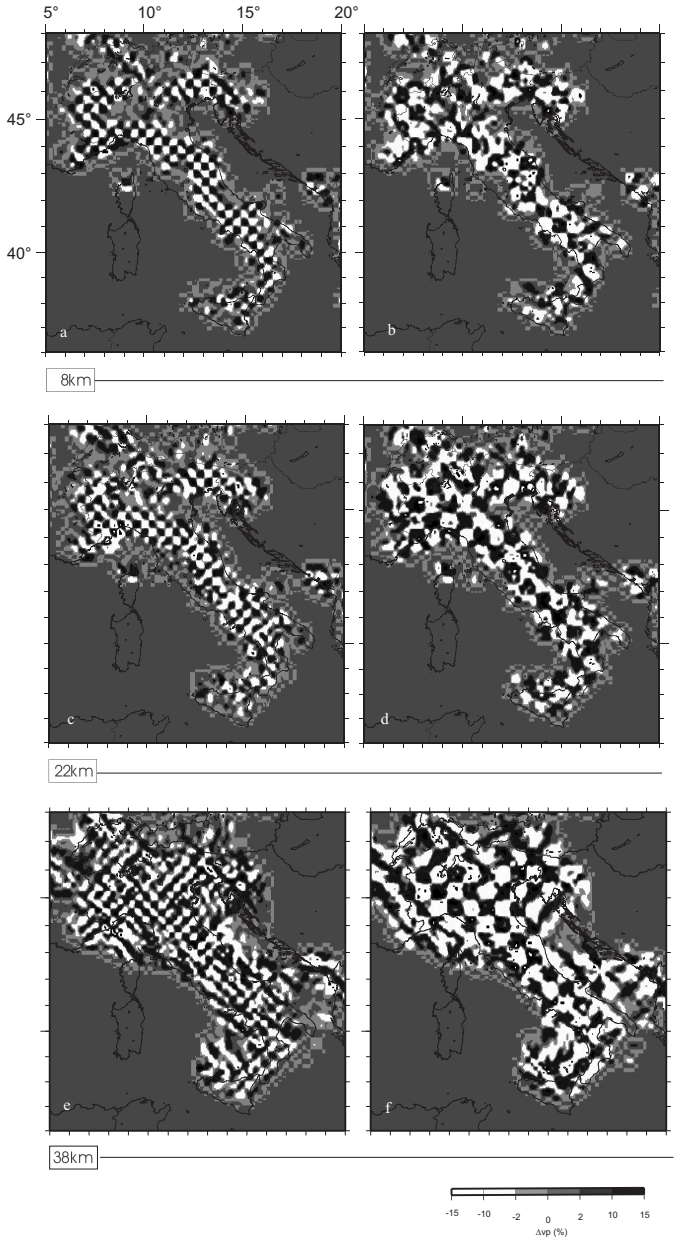

784

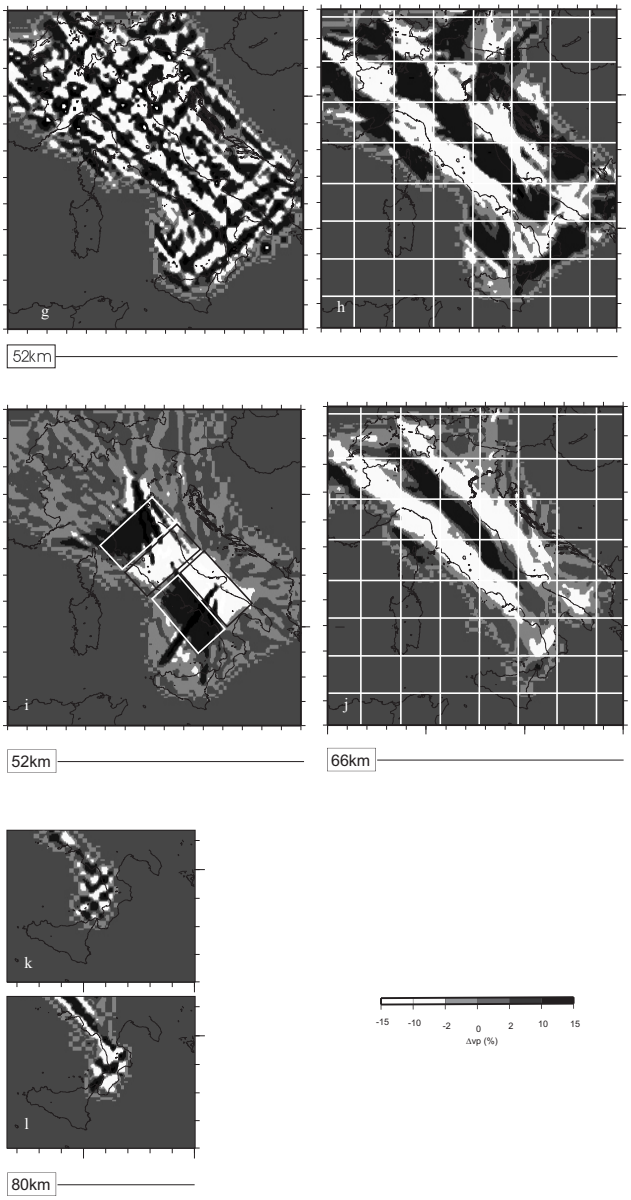

785

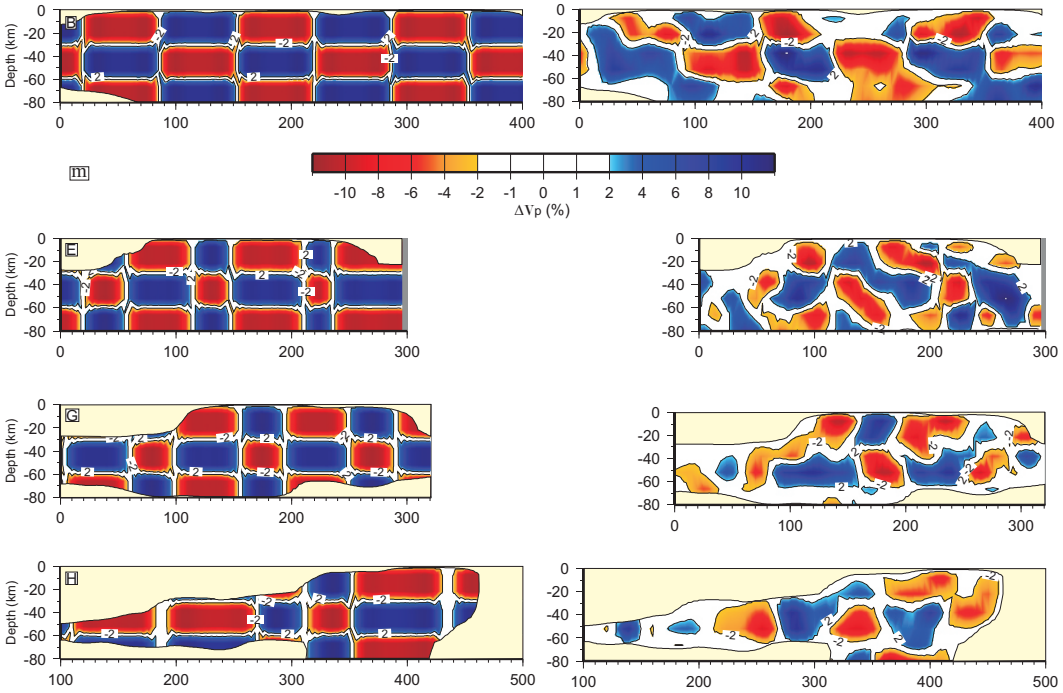
B
m
E
G
H
Depth (km)
0
-20
-40
-60
-80
0
100
200
300
400
500
-10 -8 -6 -4 -2 -1 0 1 2 4 6 8 10
ΔVp (%)

786

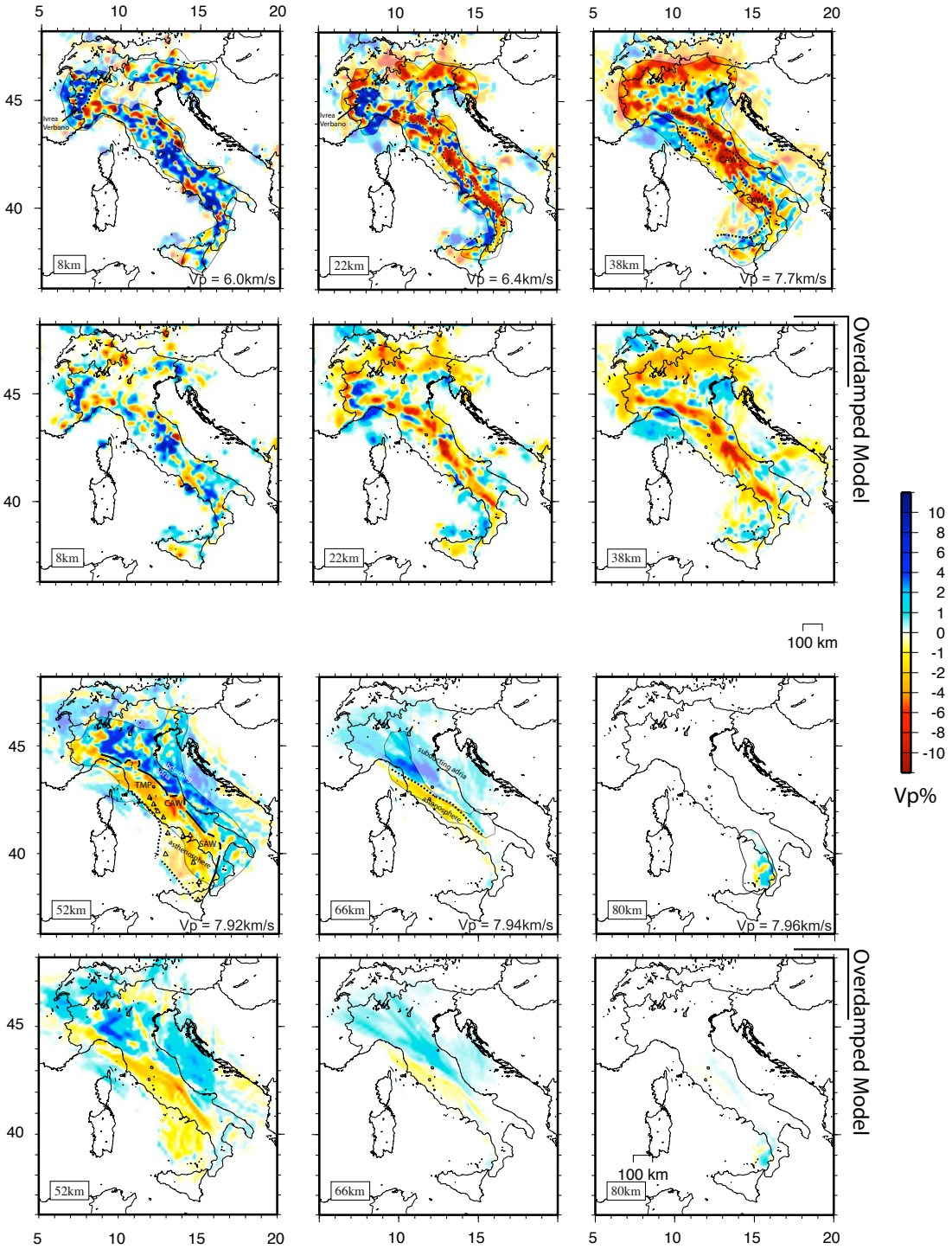
8km
Vp = 6.0km/s
22km
Vp = 6.4km/s
38km
Vp = 7.7km/s
Overdamped Model
100 km
52km
Vp = 7.92km/s
66km
Vp = 7.94km/s
80km
Vp = 7.96km/s
Vp%
10
8
6
4
2
1
0
-1
-2
-4
-6
-8
-10

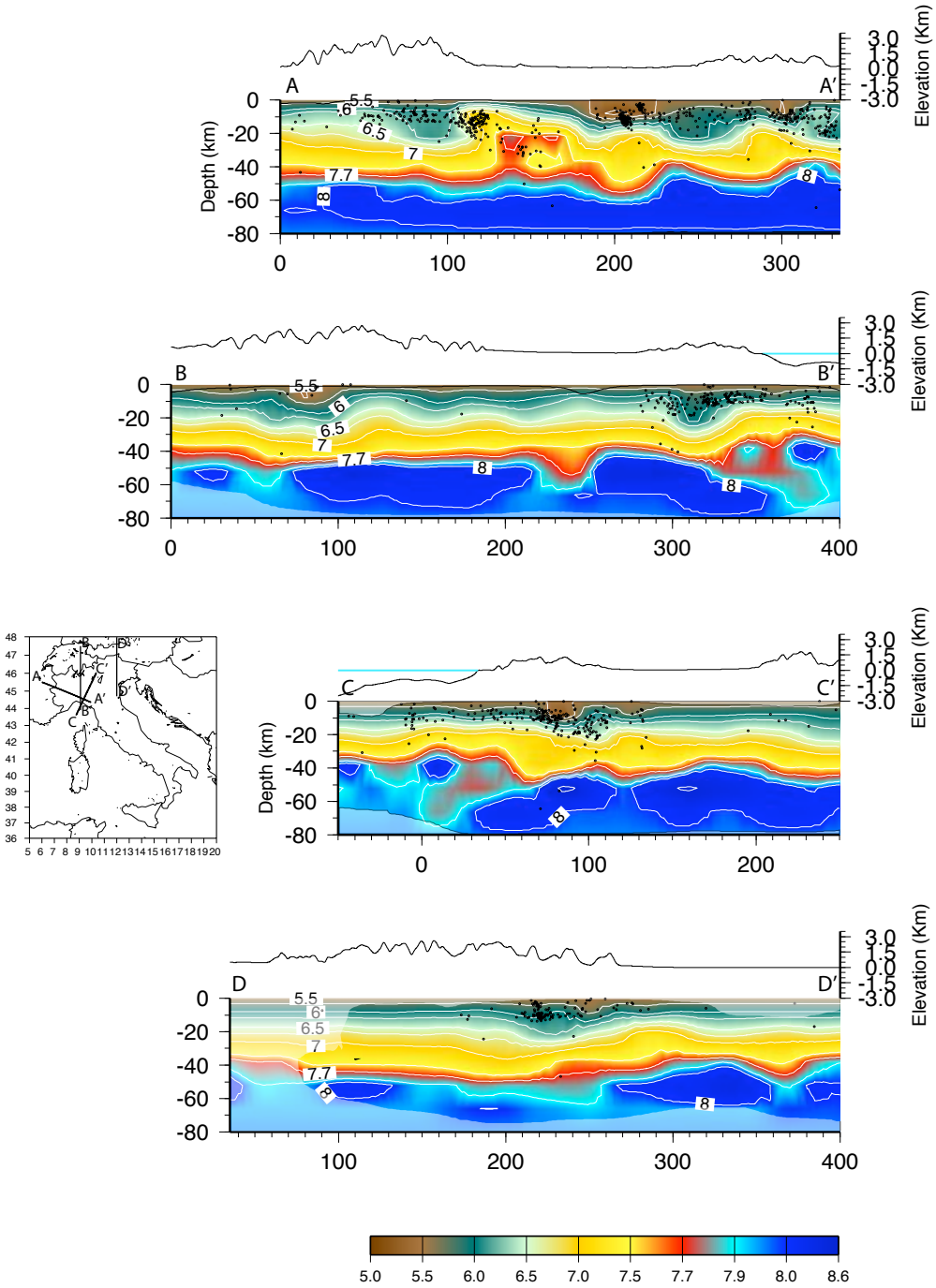

Figure 6a (Alps)

788

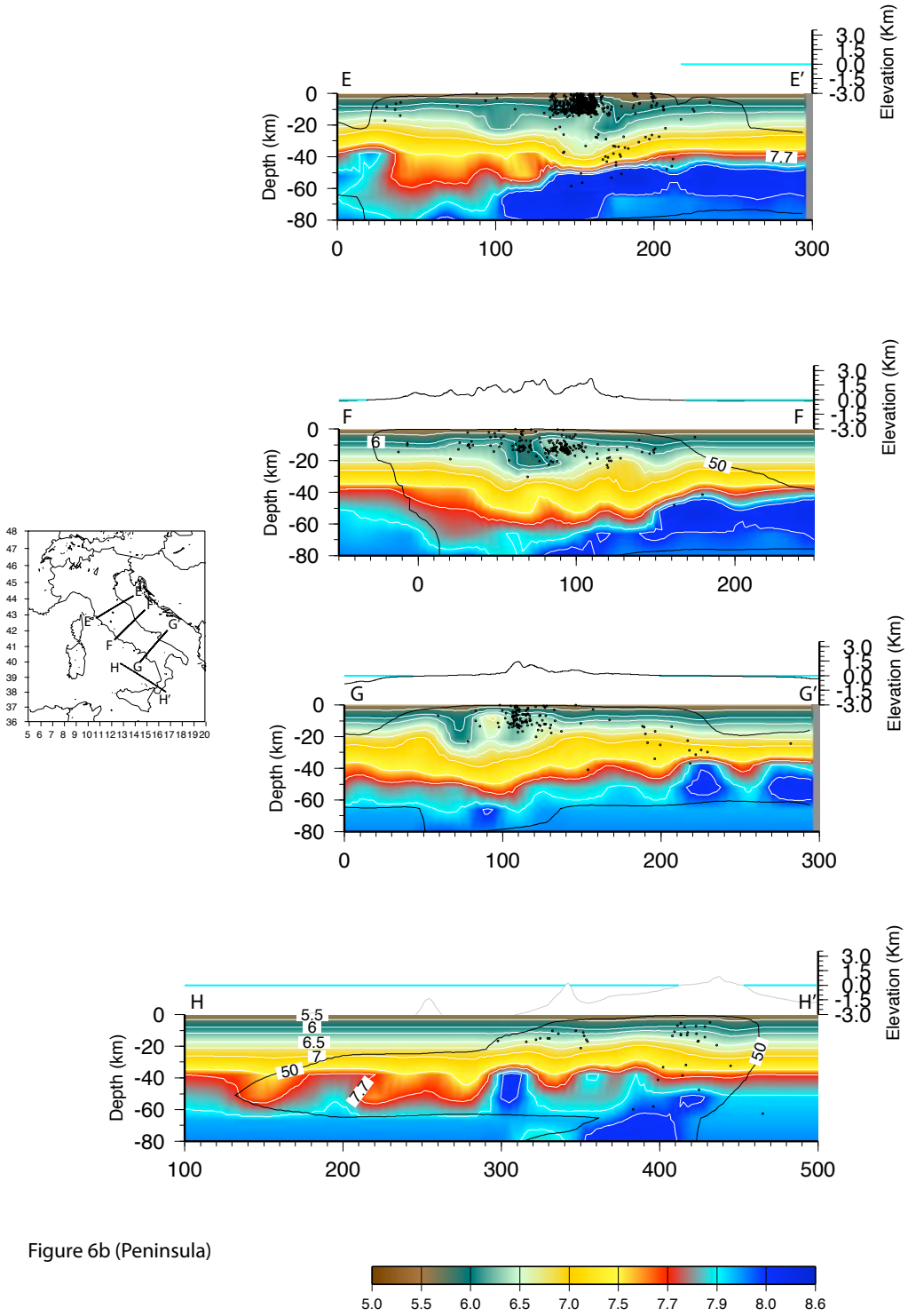

Figure 6b (Peninsula)

789

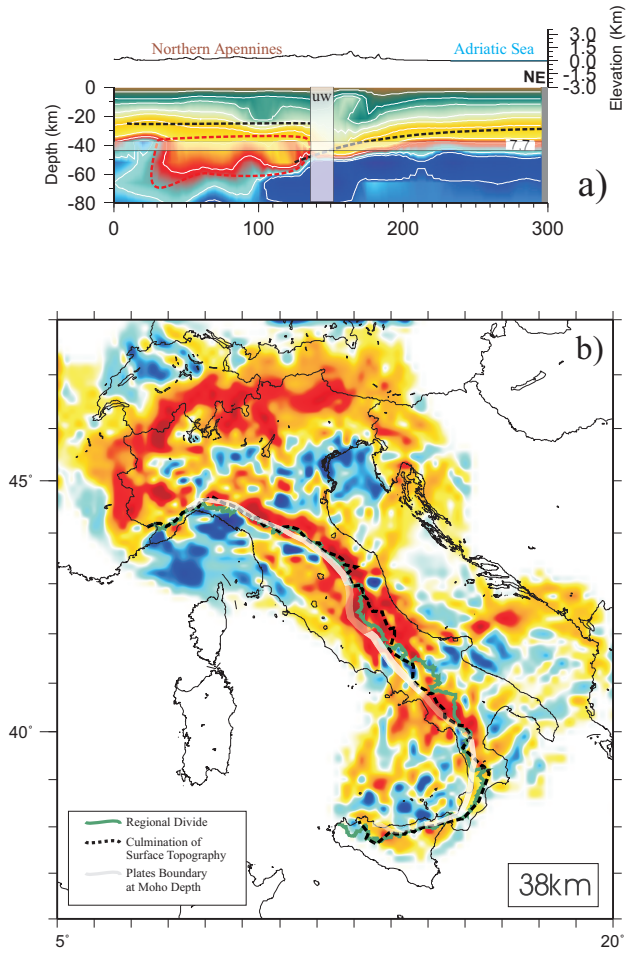
Northern Apennines
Adriatic Sea
NE
Elevation (Km)
3.0
1.5
0.0
-1.5
-3.0
Depth (km)
0
-20
-40
-60
-80
uw
7.7
a)
0
100
200
300
b)
45°
40°
5°
20°
Regional Divide
Culmination of Surface Topography
Plates Boundary at Moho Depth
38km

790

Figure 1. Map of the studied area. The red solid line traces the Adriatic-Ionian frontal thrust (modified following *Mariotti and Doglioni* [2000]). Triangles indicate volcanoes active in historical times: cf= Campi Flegrei, mv = Mt. Vesuvius, me = Mt. Etna, vu = Vulcano Island, and st = Stromboli Island. Red areas and white dashed lines indicate the main magmatic provinces of peninsular Italy and the Tyrrhenian Sea respectively: tmp = tuscan magmatic province, rmp = roman magmatic province, cmp = campanian magmatic province, vb = Mt. Vavilov Basin, mb = Mt. Marsilii Basin (modified following *Rosenbaum et al.* [2008]).

Figure 2. a) The locations of the 8206 selected earthquakes are plotted in our final 3D velocity model. The color scale represents hypocentral depth. b) The 600 permanent and temporary seismicstations belonging to INGV and other institutions. The grey scale represents the number of P-wavereadings recorded by each station.

Figure 3. a) Trade-off curves for damping parameter selection. The solid line is the rms *vs* modellength, while the dashed line is the weighted rms *vs* model length. b) The node spacing is twice the characteristic wavelength of an onset P-wave.With dashed gray lines we plot the seismic rays traced at the first iteration, based on the 1D velocity model. With black solid lines we plot the seismic rays traced at the 4^{th} iteration through a fully 3D model.

Figure 4. Resolution tests performed for synthetic structures of various sizes.For the 8km, 22km, and 38km layers: plates 1, 3 and 5 show results for 30 × 30 km squares, whileplates 2, 4 and 6 show results for 60 × 60 km squares. For the 52km layer: plate 7 showsresults for 60 × 60 km squares, plate 8 shows results for 120 × 120 km squares, and plate 9, shows results for differently oriented 120 × 240 km structures of opposite sign, separated by one model node. For the 66km layer: plate 10 shows the resolution obtained with 120 × 120 km squares. Note that the white grids in plates8 and 10 depict the geometry of the input synthetic structures. For the 80km layer:plates 11 and 12 show the resolution obtained for 30 × 30 km and 60 × 60 kmsquares respectively, in the southern Tyrrhenian sea. The resolution at this depth is goodonly within this small region. Vertical sections B, E, G, and H cut through the checkerboardsynthetic model, corresponding to the same profiles shown in Figure 6. On the left wereport the input synthetic model as a reference. Yellow masks indicate uninverted parts of themodels.

Figure 5. Tomograms of inverted layers for the preferred model and the overdamped model. Negative and positive anomalies are shown in red and blue respectively.The areas with fair to poor resolution are shaded in the preferred model. Starting P-wave velocities,in km/s, are also reported for each layer. Dashed black lines are drawn to encompass the main anomaliesdiscussed in the text. The new abbreviations are CAW = Central Apennines Window and SAW = Southern ApenninesWindow (see text). The symbols tmp, rmp, and cmp are defined in the caption of Figure 1.

Figure 6. Vertical sections through the preferred 3D velocity model. Tomograms show a continuous image of the lithosphere structure from the Alps to the Calabrian Arc.Sections B, C, and E show the V_p model along the northern segment of the EGT [*Ye et al.*, 1995], TRANSALP [*TRANSALP Working Group*, 2002], and CROP03 [*Pialli et al.*, 1998] CSS profiles. The white solid lines are contours inV_p. The black dashed lines indicate structural interpretations from other works. Dots are earthquake foci relocated in the 3D velocity model. The color palette indicates absolute V_p values in km/s.

Figure 7. Boundary between the Adriatic and the Tyrrhenian plates at Moho depth. a) An illustrative section(E in Figure 6) describing the procedure we followed to define the plate boundary with its related uncertainty (uw = uncertainty window). b) The plate boundary (light white band) along the entire peninsula, identified by analyzing vertical sections and the tomographic map at 38 km depth. Lighter segments correspondto regions where the boundary cannot be unambiguously traced (e.g., around the CAW and SAW shown inFigure 5). The regional divide (green solid line) and the culmination of surface topography(black dashed line) are also shown.